

Approximate Calculation of Time-Domain Effective Height for Aperture Antennas

Matteo Ciattaglia, *Student Member, IEEE*, and Gaetano Marrocco, *Member, IEEE*

Abstract—The time-domain (TD) effective height is a space-time vector operator recently introduced to describe the performance of ultrawide-band antennas. Since generally obtained by measurements or intensive numerical modeling, it is represented through a large set of data not very suitable to the evaluation of the whole TD link. For the particular class of aperture-radiating antennas of separable shapes, such as slot, open-ended waveguides and horns, this paper proposes a systematic TD processing of the aperture field, involving model-based deconvolution and parameter estimation, at the purpose of an efficient calculation and a more manageable representation of the effective height. Following the idea at the base of modal near to far field transformation, as previously presented by the authors, the processing of the aperture impulse response is here addressed with a particular care to the fast varying early transient. The corresponding time-dependent Radon transforms are then approximated by semi-analytical formulas whose accuracy is discussed as for the aperture size and frequency limits. The proposed methods, which are much faster than the conventional approach, are demonstrated by some examples.

Index Terms—Effective height, finite-difference time-domain (FDTD), radon transform, time domain analysis, ultrawide-band antennas, singularity expansion method (SEM).

I. INTRODUCTION

IN THE DESIGN of new ultrawide-band (UWB) applications [1] the antenna features are frequently described via the time-domain (TD) effective height [2]–[7] which plays the role of impulse response operator linking the transient radiated field to the real antenna input waveform by a convolution integral. According to the theory in [5], TD effective height is defined in terms of the Radon transform of the (electric or magnetic) antenna current impulse response. Except for a few cases, mainly concerning large antennas, [8], [9], analytical modeling is not easily achievable due to the antenna geometrical and electrical complexity. Therefore local numerical tools, and first of all the finite-difference time-domain (FDTD) method [10], are commonly used to calculate and store the TD surface current and finally, the Radon transform is evaluated numerically. Calculation and application of TD effective height is therefore a tedious and time-consuming process and produces a large four-dimensional data set. This fully numeric representation is not very suitable to be embedded within a ray tracing tool for the evaluation of the whole system performances. Instead, a TD analytical or

semi-analytical model would simplify the antenna plus channel characterization over a wide band.

At the purpose of simplifying the far-field ultrawideband description of antennas in both frequency [11] and time domain [12], the authors have recently proposed a numerical procedure, denoted as Modal-N2F, which is applicable to aperture-like radiators, such as slots, open-ended waveguides and ridged horns of separable shape. The method combines FDTD, data-fitting models and signal processing and originates a far field representation in semi-analytical formulas which are however dependent on the antenna input signal. A blind application of this method to the approximate calculation of aperture antenna effective height, although applicable, nevertheless requires a deconvolution of the transient far field and the semi-analytical representation is therefore lost. To overcome such a limitation, this paper presents a more systematic approach which is based on the calculation, and then on the process, of the aperture impulse response and still preserves the semi-analytical feature of the effective height representation. Early transient modeling of aperture impulsive field deserves particular care since this changes rapidly and spreads all over the antenna response through the convolution process and therefore cannot be neglected as in [12]. Two alternative representations of the aperture impulse responses are discussed. They involve, respectively, simpler mathematical processing and a smaller number of data to be stored. The corresponding Radon transforms for the effective height are hence derived and the pertinent early-time approximations, to obtain simplified formulas with separated time and angular variables, are discussed for the case of canonical apertures respect to the antenna size and the highest frequency of interest.

The paper is organized as follows: Section II introduces the time domain formalism for the aperture-antenna effective height; the efficient representation of impulsive TD aperture field is discussed in Section III. Formulas for numerical evaluation of TD effective height are given in Section IV and the numerical complexity is discussed in Section V. Numerical calibration and some examples are finally presented in Section VI.

II. TD APERTURE EFFECTIVE HEIGHT

An antenna with a radiating aperture S_a laying on the plane $z = 0$ (\hat{z} is the normal unitary vector on S_a) is driven through a transmission line (Fig. 1) by a real voltage generator of internal resistance R_g , which excites the input waveform $v_{in}(t)$. According to the formulation in [5], a linear-system-type representation of any antenna time-dependent far field is

$$\mathbf{E}(\mathbf{r}, t) = -\frac{1}{8\pi r c} \frac{\eta_0}{R_g} \left[v_{in}(\cdot) * \mathbf{h}^T(\hat{\mathbf{r}}, \cdot) \right] \left(t - \frac{r}{c} - t_g \right) \quad (1)$$

Manuscript received March 2, 2004; revised June 7, 2004. The work was supported in part by the Ministero dell'Università, under program PRIN-2004.

M. Ciattaglia is with the the University of Rome "Tor Vergata," 00133 Rome, Italy and also with Alenia Marconi Systems, 00131 Rome, Italy.

G. Marrocco is with the the University of Rome "Tor Vergata," 00133 Rome, Italy (e-mail: marrocco@disp.uniroma2.it).

Digital Object Identifier 10.1109/TAP.2004.842652

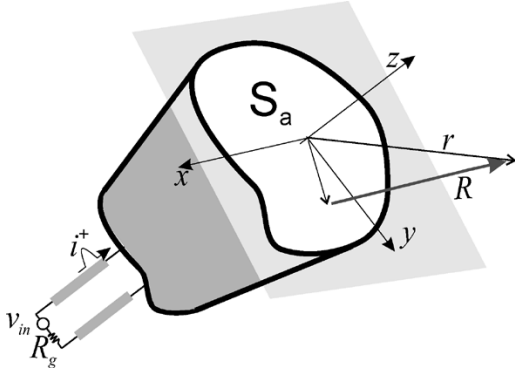


Fig. 1. Coordinate system for aperture antenna problems. A real voltage source exciting the input signal is connected to the aperture antenna (slot, open waveguide or horn) by means of a transmission line. To simplify the model, the aperture is supposed to radiate from an infinite screen.

where c is the speed of light, η_0 is the free-space impedance, t_g is the time delay along the line, “*” denotes convolution, and $\mathbf{h}^T(\hat{\mathbf{r}}, \tau)$ is the TD antenna effective height in transmitting mode.

Denoting with $\mathbf{E}_a^\delta(\boldsymbol{\rho}, \tau)$ (units in $[\Omega m^{-1} s^{-1}]$) the tangential component of aperture field corresponding to a Dirac-pulse input current, the TD effective height of the aperture (see Appendix A for details), supposed to radiate from an infinite screen, is

$$\mathbf{h}^T(\hat{\mathbf{r}}, \tau) = 2 \left[-\frac{1}{\eta_0} \hat{\mathbf{r}} \times \iint_{S_a} \mathbf{E}_a^\delta \left(\boldsymbol{\rho}, \tau + \frac{\hat{\mathbf{r}} \cdot \boldsymbol{\rho}}{c} \right) ds \times \hat{\mathbf{z}} \right] * \delta^{(1)}(\tau) \quad (2)$$

where, for simplicity, it has been supposed $t_g = 0$. The function $\delta^{(1)}(\tau) = (\partial/\partial\tau)\delta(\tau)$ accounts for the derivative effect on the input signal. The Radon transform within square brackets (units in m/s) is the effective height in the receiving mode, $\mathbf{h}^R(\hat{\mathbf{r}}, \tau)$.

The knowledge of TD effective height requires the application of a local method, such as FDTD, to calculate the aperture field when the antenna is sourced by a broadband test signal $v_0(t)$, typically a Gaussian pulse, since the Dirac pulse is not suitable as input signal for numerical codes. The corresponding aperture field $\mathbf{E}_a(\boldsymbol{\rho}, t)$ has to be stored within the whole transient and numerical deconvolution is then applied to each aperture radiating pixel to calculate the impulse response $\mathbf{E}_a^\delta(\boldsymbol{\rho}, \tau)$. Finally, the effective height is obtained by numerical evaluation of surface integral in (2) which has to be repeated at any required time and observation direction because of the coupling between angular and spatial variables. The numerical effective height will be a baseband approximation, within the band of $v_0(t)$, of the true effective height.

III. NUMERICAL REPRESENTATIONS OF THE APERTURE IMPULSE RESPONSE

A great simplification in the above numerical procedure is achieved in this paper by introducing an approximated space-time uncoupling model of the impulsive aperture field $\mathbf{E}_a^\delta(\boldsymbol{\rho}, \tau)$

$$\mathbf{E}_a^\delta(\boldsymbol{\rho}, \tau) \approx \sum_{p=1}^N g_p(\tau) \mathbf{e}_p(\boldsymbol{\rho}) \quad (3)$$

$\{\mathbf{e}_p(\boldsymbol{\rho})\}$ are time-independent aperture basis functions, here the transverse eigenvectors (modes) of the waveguide having S_a cross-section. $\{g_p(\tau)\}$ (units in $[\Omega/s]$) are unknown time-variant coefficients, hereafter denoted as *scalar impulse responses*, which have to be computed numerically from the aperture field \mathbf{E}_a excited by v_0 . At this purpose, the computed \mathbf{E}_a is fitted, at run-time, onto the same basis by coefficients $\gamma_p(t)/2R_g = \int \int_{S_a} \mathbf{E}_a(\boldsymbol{\rho}, t) \cdot \mathbf{e}_p(\boldsymbol{\rho}) ds$. The unknown scalar impulse responses are finally obtained by deconvolution of scalar functions instead of surface vector functions

$$\gamma_p(t) = \int_0^t g_p(t - \tau) v_0(\tau) d\tau. \quad (4)$$

The solution of above integral equation in a form suitable for the calculation of the effective height in (2) is achieved by introducing two different models of scalar impulse response $g_p(\tau)$ within the hypothesis that the test signal $v_0(t)$ is a practically time-limited excitation signal in $[0, T_0]$. The first model, denoted as *complete fitting* (CF) model gives a more efficient representation of the early transient, while the second one, referred to as *incomplete fitting* (IF) model, is less accurate in the early transient but permits to derive simple semi-analytical expressions for the TD effective height.

A. CF Model

According to the singularity expansion method (SEM) [13], the response of an electromagnetic system to a time-limited excitation can be represented by a superposition of damped oscillating functions, which describe the late transient, and an entire function accounting for the early transient. Therefore, the following model for the scalar impulse responses $g_p(\tau)$ is introduced:

$$g_p^{\text{CF}}(\tau) \approx g_{p,\infty} \delta(\tau - t_p) + \sum_{k=-K_p}^{K_p} g_{pk} e^{s_{pk} \tau} U(\tau - t_p) \quad (5)$$

where the shifted Dirac-pulse and the corresponding real-valued $g_{p,\infty}$ coefficient describe the instantaneous effect of the driving voltage source on the aperture modes. The complex poles and residues $\{s_{pk}, g_{pk}\}$ take into account the oscillating contributes due to the complex natural resonances of the source, and multiple diffractions by the guiding section (or cavity) and by the aperture.

Introducing (5) in (4)

$$\gamma_p(t) = g_{p,\infty} v_0(t - t_p) + \sum_k g_{pk} e^{s_{pk} t} \times \int_0^{T_0} e^{-s_{pk} \tau} v_0(\tau) U(t - \tau - t_p) d\tau. \quad (6)$$

Although the averaged delay time t_p is estimated numerically as shown later on, it is first assumed that $t_p \approx z_A/c$ where z_A is the distance of the source point from the aperture center.

The impulse response parameters are calculated by a two-steps procedure. First, poles and residues $\{g_{pk}, s_{pk}\}$ are computed from the late transient of shifted signal $\gamma_p(t - (z_A/c) - T_0)$ by the method in [14]. Then the coefficients of the Dirac functions are estimated by processing of γ_p within the early time

interval $(z_A/c) < t' < (z_A/c) + T_0$. Denoting with $\gamma_p^{(p)}(t')$ the poles's contribute to γ_p

$$\gamma_p^{(p)}(t') = \sum_k g_{pk} e^{s_{pk} t'} \int_0^{t' - \frac{z_A}{c}} e^{-s_{pk} \tau} v_0(\tau) d\tau \quad (7)$$

the *nonpole* contribute is calculated as $\gamma_p^{(np)}(t') = \gamma_p(t') - \gamma_p^{(p)}(t')$. Parameters $\{t_p, g_{p,\infty}\}$ are hence evaluated by best fitting of $\gamma_p^{(np)}(t')$ to $g_{p,\infty} v_0(t' - t_p)$. In particular, a refinement of t_p is such to maximize the correlation $\int_p \gamma_p^{(np)}(t') v_0(t' + t_p) dt'$ and parameter $g_{p,\infty}$ is then calculated by least square method. However, numerical simulations have shown that the estimated delay t_p is nearly coincident with z_A/c .

B. IF Model

A simplified representation of the scalar impulse response, $g_p^{\text{IF}}(\tau)$, can be obtained by using only the complex exponentials set. However poles and residues are now expected to be different than the corresponding parameters of the CF-model. The IF expansion is extremely fast convergent in the late transient, while a larger number of exponentials are required to fit the very early transient.

The fitting parameters are computed by a different procedure. The scalar impulse response $g_p(\tau)$ is numerically deconvolved from (4) by the fourth-order moment expansion (ME) deconvolution [15] and then $g_p(\tau)$ is fitted on $g_p^{\text{IF}}(\tau)$ for $\tau > t_p$ by means of the matrix pencil method [16].

In both the deconvolution schemes, the set of poles and residues to be really retained and stored for the calculation of the radiated field can be thinned according to the strength of the *energy* indicator [12]. In particular, only poles with energy higher than one per thousand of the maximum energy will be retained for the effective height computation.

IV. APPROXIMATE CALCULATION OF TD EFFECTIVE HEIGHT

Consider first the CF-model of the impulsive aperture field, by combining (5) with (3) and (2), the effective height is there written in the following approximate form:

$$\mathbf{h}^T(\hat{\mathbf{r}}, \tau) = 2 \sum_{p=1}^N \left\{ g_{p,\infty} \mathbf{h}_{p,\infty}^R(\hat{\mathbf{r}}, \tau) + \sum_{k=-K_p}^{K_p} g_{pk} \mathbf{h}_{pk}^R(\hat{\mathbf{r}}, \tau) \right\} * \delta^{(1)}(\tau) \quad (8)$$

where the following integrals need to be solved:

$$\begin{bmatrix} \mathbf{h}_{p,\infty}^R(\hat{\mathbf{r}}, \tau) \\ \mathbf{h}_{pk}^R(\hat{\mathbf{r}}, \tau) \end{bmatrix} = -\frac{1}{\eta_0} \hat{\mathbf{r}} \times \iint_{S_a} \left[U\left(\tau - t_p + \frac{\hat{\mathbf{r}} \cdot \boldsymbol{\rho}}{c}\right) e^{s_{pk}(\tau + \frac{\hat{\mathbf{r}} \cdot \boldsymbol{\rho}}{c})} \right] \mathbf{e}_p(\boldsymbol{\rho}) ds \times \hat{\mathbf{z}}. \quad (9)$$

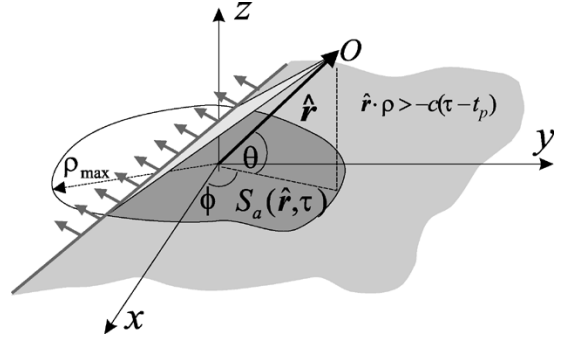


Fig. 2. Portion $S_a(\hat{\mathbf{r}}, \tau)$ of the aperture whose radiation contributes at times $\tau < t_p + (\rho_{\max}/c)$ to the effective height at observation direction $\hat{\mathbf{r}}$.

A trivial solution can be obtained at boresight radiation (e.g. $\theta = 0$, and $\hat{\mathbf{r}} \cdot \boldsymbol{\rho} = 0$) where the angular and temporal variables are fully decoupled. In this case it is easy to prove that the effective height can be expressed, for both CF- and IF-model, as

$$\mathbf{h}^T(\tau) = 2 \sum_{p=1}^N \mathbf{e}_p^{(0)} g_p(\tau) * \delta^{(1)}(\tau). \quad (10)$$

The constant vector $\mathbf{e}_p^{(0)} = -(1/\eta_0) \hat{\mathbf{r}} \times \int \int_{S_a} \mathbf{e}_p(\boldsymbol{\rho}) ds \times \hat{\mathbf{z}}$ is calculated exactly for canonical apertures such as rectangular and circular and vanishes for odd aperture patterns.

In the more general case of off-boresight observation, $\mathbf{h}_{p,\infty}^R$ is transformed into a line integral applied to the basis function $\mathbf{e}_p(\boldsymbol{\rho})$ along a time varying boundary by the properties of Dirac functions, as discussed in Appendix B, for the particular case of rectangular apertures. Concerning the integral \mathbf{h}_{pk}^R , it can be observed that the presence of Heaviside function $U(\tau - t_p + (\hat{\mathbf{r}} \cdot \boldsymbol{\rho}/c))$ accounts for the very early transient when only the portion $S_a(\hat{\mathbf{r}}, \tau)$ of the aperture, intercepted by the half-plane $\tau - t_p + (\hat{\mathbf{r}} \cdot \boldsymbol{\rho}/c) > 0$, gives contribution to the observation point (see Fig. 2). After a time $\tau > t_p + (\rho_{\max}/c)$, ρ_{\max} being the maximum distance between aperture rim and its center, the observation point starts to collect radiation from the whole aperture and the Heaviside function approach to unity. Integral \mathbf{h}_{pk}^R can be therefore decomposed as in (11), shown at the bottom of the page, where $\mathbf{F}_{pk}(\hat{\mathbf{r}})$ is the p th modal space factor, e.g., the spectral Fourier transform of the p th aperture field pattern evaluated at singular frequency $\omega = -js_{pk}$ and it is known in closed form for both rectangular and circular apertures [12]. The numerical integration of \mathbf{h}_{pk}^R is therefore only required within the very short time interval ρ_{\max}/c which leads to a modest increase in the computational effort compared with a true closed form. However, exact integrals, just like \mathbf{F}_{pk} , can be derived even in the very early transient for the principal cuts $\phi = \{0, \pi/2\}$, at least for rectangular apertures

For the case of IF-model of the aperture, field only integrals $\mathbf{h}_{pk}^R(\hat{\mathbf{r}}, \tau)$ need to be solved for off-boresight radiation. However, it is interesting to discuss within which condition the closed form expression, appearing in the lower branch of (11),

$$\mathbf{h}_{pk}^R(\hat{\mathbf{r}}, \tau) = -\frac{1}{\eta_0} \begin{cases} \hat{\mathbf{r}} \times e^{s_{pk} \tau} \iint_{S_a(\hat{\mathbf{r}}, \tau)} e^{s_{pk}(\frac{\hat{\mathbf{r}} \cdot \boldsymbol{\rho}}{c})} \mathbf{e}_p(\boldsymbol{\rho}) ds \times \hat{\mathbf{z}}, & \text{if } |\tau - t_p| \leq \frac{\rho_{\max}}{c} \\ \cos \theta \mathbf{F}_{pk}(\hat{\mathbf{r}}) e^{s_{pk} \tau}, & \text{if } \tau > t_p + \frac{\rho_{\max}}{c} \end{cases} \quad (11)$$

TABLE I
 COMPUTATIONAL COSTS OF MAIN PROCESSING TASKS

Task	Complexity
Deconv. of $\mathbf{E}_a^\delta(\boldsymbol{\rho}, \tau)$	$2O^{DE}(N_t)N_c$
Deconvolution of $g_p(\tau)$	$O^{DE}(N_t)N$
Calculation of Radon Transform	$2N_a N_t N_c$
Modal decomposition on the aperture	$2N N_t N_c$
Parameter estimation (SVD)	$O^{SVD}(N_{t1})N$
Early-time calculation of \mathbf{h}_{pk}^R	$2N N_{t2} N_a N_c$
Early-time calculation of $\mathbf{h}_{p,\infty}^R$	$2N \sqrt{N_c} N_{t2} N_a$

may be used as *early-time extrapolator* also within the interval $|\tau - t_p| \leq (\rho_{\max}/c)$ therefore avoiding the numeric evaluation of the integral on the time-dependent surface $S_a(\hat{\mathbf{r}}, \tau)$. In this case the effective heights can be simply calculated with full separation of time and angular variables as

$$\mathbf{h}^R(\hat{\mathbf{r}}, \tau) = -\frac{1}{\eta_0} \cos\theta \sum_{p,k} g_{pk} \mathbf{F}_{pk}(\hat{\mathbf{r}}) e^{s_{pk}\tau} \quad (12)$$

and $\mathbf{h}^T(\hat{\mathbf{r}}, \tau) = 2\mathbf{h}^R(\hat{\mathbf{r}}, \tau) * \delta^{(1)}(\tau)$. Since the above approximation only interests the very early transient, it will mainly affect the high frequency content of the effective height and its accuracy is expected to depend on the aperture size ρ_{\max} . It is therefore reasonable that, for a given ρ_{\max} , the early-time extrapolation will be accurate up to a maximum frequency f_{\max} and the following heuristic guideline for the extrapolation usage is assumed:

$$\rho_{\max} f_{\max} \leq Kc \quad (13)$$

where c is the speed of light and K a constant. This expression will be verified by numeric analysis in the next section.

V. DISCUSSION ABOUT NUMERICAL COMPLEXITY

The numerical complexity of the proposed method, compared with the standard calculation which involves the deconvolution of the aperture field and then the numerical Radon transform, is here discussed. The following notation is adopted: N_t means the number of FDTD time samples of the antenna response, N_c the number of space samples on the aperture, N_a the number of observation angles and again N the number of basis functions on the aperture. The main processing tasks that will be considered for the CF- and IF-modes evaluation are the modal decomposition, the deconvolution of scalar impulse responses, the Matrix Pencil method, which is essentially based on the SVD, and the numerical calculation of time-dependent integrals in (9) and (11) by finite summations. Relevant computational costs are listed in Table I.

The numerical complexity of deconvolution (having supposed to adopt fourth-order ME as in [15]) is $O^{DE}(N_t) = 4N_t$; the SVD complexity is [17] roughly $O^{SVD}(N_{t1}) = (N_{t1}/2)^3$ where $N_{t1} = N_t/n_d$ denotes a resampled set of the FDTD oversampled data (generally $n_d = 3 \div 5$); $N_{t2} \approx (2\rho_{\max}/c) \approx$

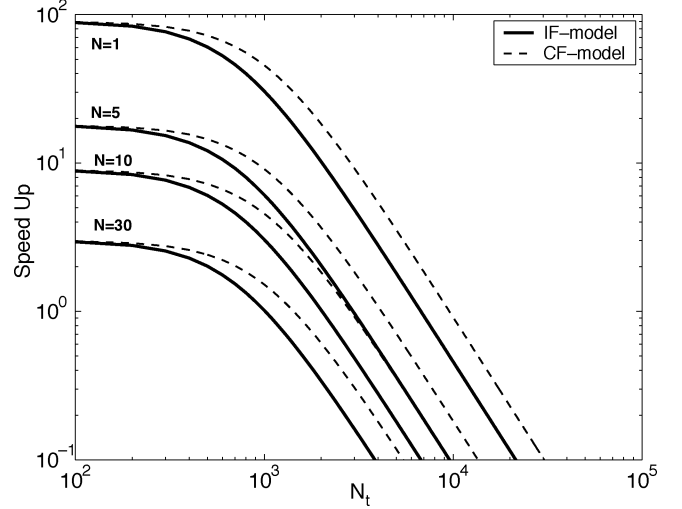


Fig. 3. Speed-up of the proposed methods in the calculation of the effective height along a single angular cut with 2° increments ($N_a = 90$) and typical values $N_c = 10^3$, $n_d = 4$.

$\sqrt{N_c}/c$ is the number of early-time samples. By simple mathematical manipulations and some approximations, the following expressions for the complexity are obtained:

$$O^{ST} = 2N_a N_c N_t \quad (14)$$

$$O^{CF} = N \left[2N_t N_c + \frac{N_t^3}{8n_d^3} + \frac{2N_a N_c^{\frac{3}{2}}}{c} \right] \quad (15)$$

$$O^{IF} = 2N \left[N_t N_c + \frac{N_t^3}{8n_d^3} + N_a N_c^{\frac{3}{2}} \right] \quad (16)$$

where O^{ST} is for the complexity of the standard method. The speed-up of the two proposed procedures respect to standard calculation, namely $SU^{CF} = O^{ST}/O^{CF}$ and $SU^{IF} = O^{ST}/O^{IF}$, are represented in Fig. 3 versus the number of time samples, for typical parameters' values. It can be observed that the benefit of the CF- and IF-models are as much relevant as the number of the required aperture basis functions is small. The CF-model appears more efficient than the IF-model, even for a same number of aperture functions, since it avoids the numerical deconvolution by ME and permits to perform deconvolution and parameters' estimation within a same task. The speed-up gets worse, in both the models, as the number of time samples increases due to the larger computational time wasted in the aperture field expansion. However, for typical 10^3 time samples and $N = 5$, the speed-up is about 10 for both the methods. Much more relevant benefits are achieved when the effective height needs to be evaluated at a larger set of angles.

VI. NUMERICAL ANALYSIS

A. Radiation From a Rectangular Aperture

A rectangular $a \times b$ slot on a perfect electric screen is excited by a dipole placed in front of the aperture (inset in Fig. 4). The structure has been meshed on a uniform rectangular FDTD grid, with voxel size $\Delta = 0.5$ cm, which includes the antenna and a small region in the close surrounding of the aperture. Denoting with $f^{\text{FDTD}} = c/(10\Delta) = 6$ GHz the maximum frequency

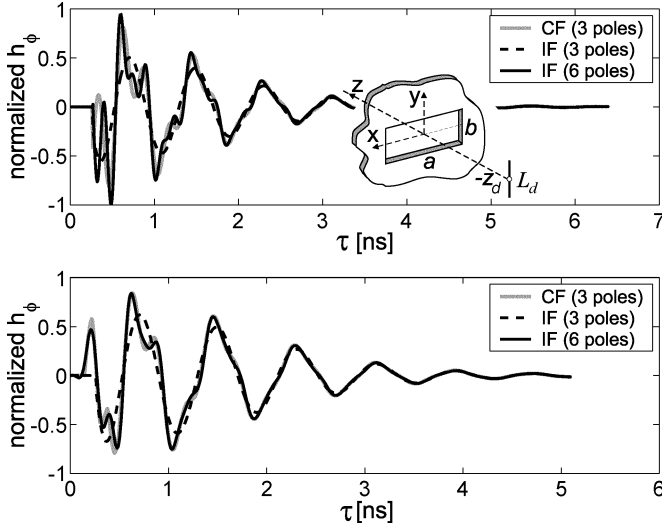


Fig. 4. Characterization of a dipole-fed rectangular slot: size (in centimeters) $a = 10$, $b = 5$, $L_d = 11.5$, $z_d = 8$. Effective height in transmitting mode along the boresight (up) and (down) off the boresight at $\theta = 42^\circ$, $\phi = 45^\circ$. Dirac pulses at $\tau = t_p \approx z_A/c$ are not shown.

permitted by a such FDTD grid, the dipole has been sourced by a test Gaussian signal $v_0(t) = e^{-(t-a)^2/2\beta^2}$ whose parameters α , β , are adjusted so that the frequency f_{\max} , where the spectrum amplitude $|V_0(f)|$, ($V_0(f)$ is the Fourier transform of $v_0(t)$), attenuates to the 10% of its maximum value (in symbols: $|V_0(f_{\max})| = (1/10) \max |V_0(f)|$) is exactly f^{FDTD} . Accordingly, the effective height computed by means of the proposed methods will permit to process only those input signals $v_{\text{in}}(t)$ whose spectrum is within $[0, f^{\text{FDTD}}]$.

To obtain $\mathbf{h}(\hat{\mathbf{r}}, \tau)$ parameters, the transient aperture field has been then processed by the proposed methods, involving both CF- and IF-models. The only TE_{10} mode has been considered for the effective height calculation. Results mainly differ (Fig. 4) in the early transient where the IF-model requires a larger number of poles.

To discuss the accuracy of the effective height formulas depending on the number of poles used in the TD model of the impulsive aperture field, the transient electric far field, denoted with $E^{\text{conv}}(\mathbf{r}, t)$, has been calculated by means of the convolution in (1) when the input signal is a Gaussian pulse with $f_{\max} = 4.5$ GHz (e.g. within the numerical effective height band). That field is compared with a reference solution, denoted with $E^{\text{FDTD}}(\mathbf{r}, t)$, obtained, here and in the next examples, by an independent time-consuming FDTD simulation sourced by $v_{\text{in}}(t)$ and extending within a larger domain including also the far field test points. The following instantaneous error at observation point \mathbf{r}_0 for the E_ϕ component has been further considered:

$$\delta E(\mathbf{r}_0, t) = \frac{|E_\phi^{\text{FDTD}}(\mathbf{r}_0, t) - E_\phi^{\text{conv}}(\mathbf{r}_0, t)|}{\|E_\phi^{\text{FDTD}}(\mathbf{r}_0, t)\|_\infty}. \quad (17)$$

As expected, the error is higher in the early transient and decreases as the time goes on (Fig. 5). Moreover, CF-model's outcomes are more accurate than those obtained with IF-model which requires a larger number of poles to guarantee the same

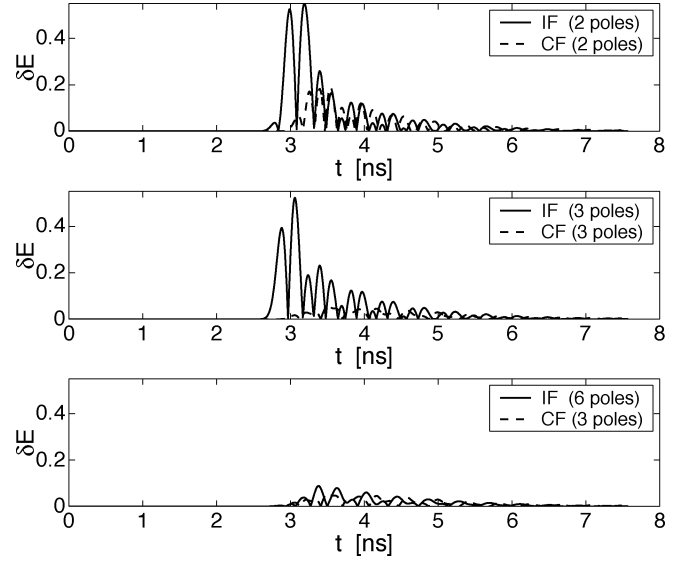


Fig. 5. Radiation from the dipole-slot system: instantaneous error in the far field calculation, at point ($r = 74$ cm, $\theta = 42^\circ$, $\phi = 45^\circ$), for an input Gaussian pulse with 10%-frequency of 4.5 GHz. The convolution equation in (1) has been applied for different orders of CF- and IF-models.

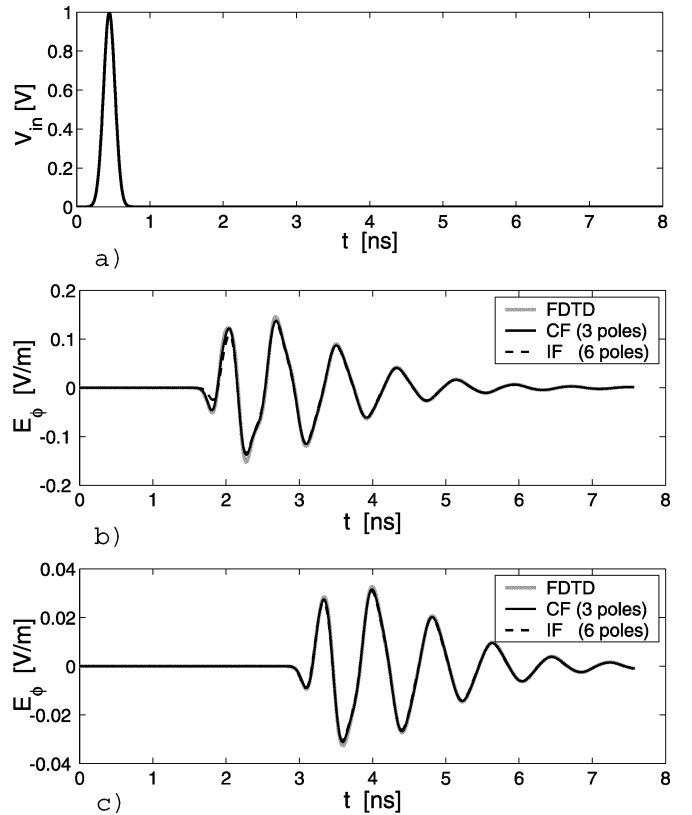


Fig. 6. Radiation from a dipole-slot system: (a) input Gaussian pulse sourcing the dipole with highest frequency $f_{\max} = 4.5$ GHz. Comparison of far field at (b) point ($r = 35$ cm, $\theta = 0^\circ$, $\phi = 0^\circ$) and (c) point ($r = 74$ cm, $\theta = 42^\circ$, $\phi = 45^\circ$) obtained by full FDTD analysis and convolution between v_{in} and the numerical effective height.

accuracy. In particular, by using 3 and 6 poles for the CF and IF model, respectively, the estimated radiated field compares well (Fig. 6) with the reference solution.

In a further experiment, the accuracy degradation of the simplified IF-model caused by the early-transient approximation,

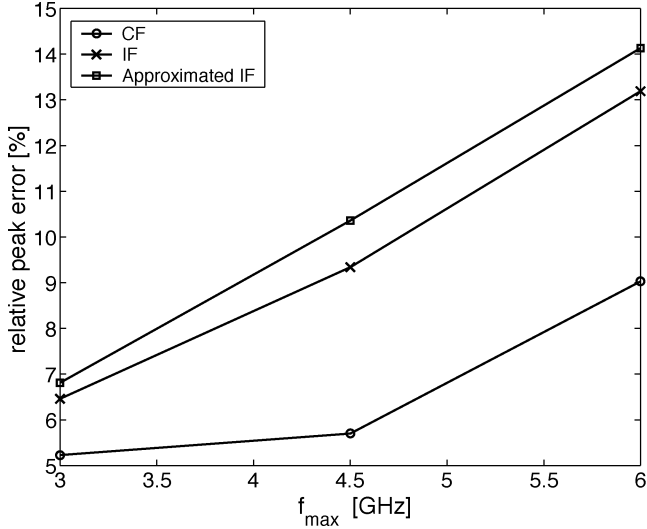


Fig. 7. Radiation from a rectangular slot: relative peak error for different input Gaussian signals of upper frequencies f_{\max} and different models of effective height.

e.g., by the direct use of the semi-analytical formula (12), is investigated. To this purpose a set of input Gaussian pulses with different maximum frequencies $f_{\max} = \{3, 4, \text{ and } 6 \text{ GHz}\}$ are convolved with the effective height computed by the different models and compared with the corresponding reference solutions. In particular, only the early transient $t < (z_A + r/c) + (3\rho_{\max}/2c)$ ($\rho_{\max} = \sqrt{a^2 + b^2}/2 = 5.6 \text{ cm}$) is considered for an off-boresight observation point and the relative peak error $\delta \tilde{E}(\mathbf{r}_0) = \max_t \delta E(\mathbf{r}_0, t)$ is evaluated. As depicted in Fig. 7, errors increase with the upper frequency of the input signal and the accuracy of the extrapolated IF effective height is a few points worse than the conventional complete model. The maximum frequency of the input signal up to which the further simplified effective height in (12) still applies with an accuracy comparable to the true IF-model, is hence chosen such that the error difference with that model exceeds 1%. The heuristic guideline in (13) is hence verified with $f_{\max} = 4.5 \text{ GHz}$, and therefore $K \simeq 0.85$. The early time extrapolation within $|\tau - t_p| \leq \rho_{\max}/c$, by the simplified IF formula (12), can be therefore roughly applicable up to frequency $f \leq c/\rho_{\max}$.

B. UWB Ridged Pyramidal Horn

The proposed method is now applied to characterize the effective height of a wideband pyramidal ridged horn. The transmitting effective height computed in the band $[0 - 6.5 \text{ GHz}]$ is shown in Fig. 8 at two different observation angles. The estimated delay time t_p is nearly identical to z_A/c ($t_p = 1.11 \text{ ns}$ for the TE_{10} mode and $z_A/c = 1.12 \text{ ns}$). Also in this case the simplified IF-model in (12) is still able to extrapolate the not negligible effective height oscillations in the very early time.

As an example of how the computed effective height can be useful in the evaluation of real transmitted signal distortion, the following excitation signal for the horn antenna is considered: $v_{\text{in}}(t) = x_{\text{DG}}(t) - (1/2)x_{\text{DG}}(t - 1.6 \text{ ns})$, where x_{DG} is a derivated Gaussian pulse, $x_{\text{DG}}(t) = (t - \alpha/\beta) \exp(-(t - \alpha)^2/(2\beta^2))$, with maximum frequency (defined as in the previous example) $f_{\max} = 3.5 \text{ GHz}$ (Fig. 9). The corresponding

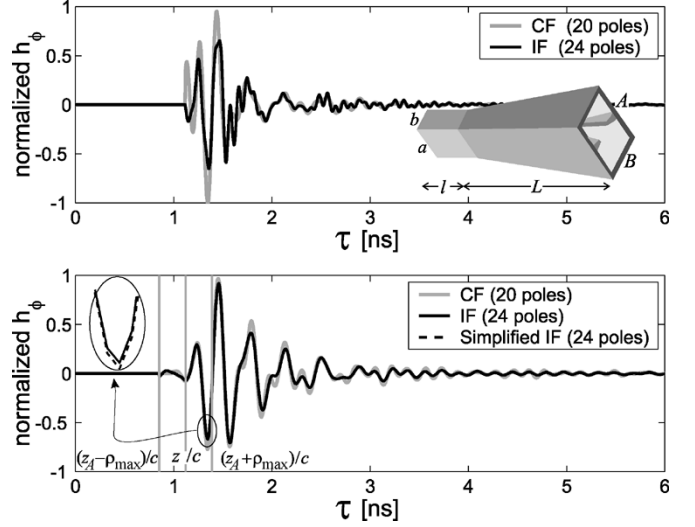


Fig. 8. Pyramidal ridged-horn (sizes in centimeters: $a = 7.75$, $b = 3$, $l = 3.6$, $A = 13$, $B = 9.25$, $L = 30.4$): transmitting-mode effective height calculated by the CF and IF-model with different numbers of poles corresponding to a threshold thinning of 10^{-3} ; (top) observation at the aperture boresight; (bottom) observation at $(\theta = 30^\circ, \phi = 0^\circ)$. Dirac pulses at $\tau \approx z_A/c$ are not shown.

radiated field has been computed via the convolution in (1) with the effective height. Comparisons in Fig. 9 show a good agreement between reference solution and the data computed by the new method provided that 20 and 24 pole-residue couplets are used for CF- and IF-model respectively.

VII. CONCLUSION

This paper has addressed the approximate numerical calculation of TD effective height for real aperture-radiating antennas. The proposed method is a fully automated combined procedure involving a local electromagnetic solver and signal processing for the manipulation of the aperture impulse response. By the use of two alternative time- and space-fitting models, the burden of the effective height computation has been greatly reduced to more than an order of magnitude, since the numerical solution of the Radon transform is restricted only within a very short time, depending on the aperture size. Anyway, analytical expressions have been derived for observation along the antenna boresight and along the principal planes. Within a discussed frequency limitation, a further approximated formula permits, for the case of IF-model, to obtain the effective height at any observation direction without calculation of integrals. The complete spatial and temporal filtering behavior of the antenna is therefore captured by a small set of parameters, depending on the antenna geometry and on the frequency range of interest.

Although only demonstrated for rectangular apertures, the method can be immediately applied to circular shapes, for which exact far field expressions are already available and, in principle, even to different kinds of apertures, provided that suitable vector or scalar basis functions, with known spectral Fourier transform, could be defined.

The numerical procedure is mainly a post-processing and hence it is suited to strengthen any existing TD numerical solver, e.g., without the need to affect the electromagnetic computation core. Due to the simplicity of the effective height

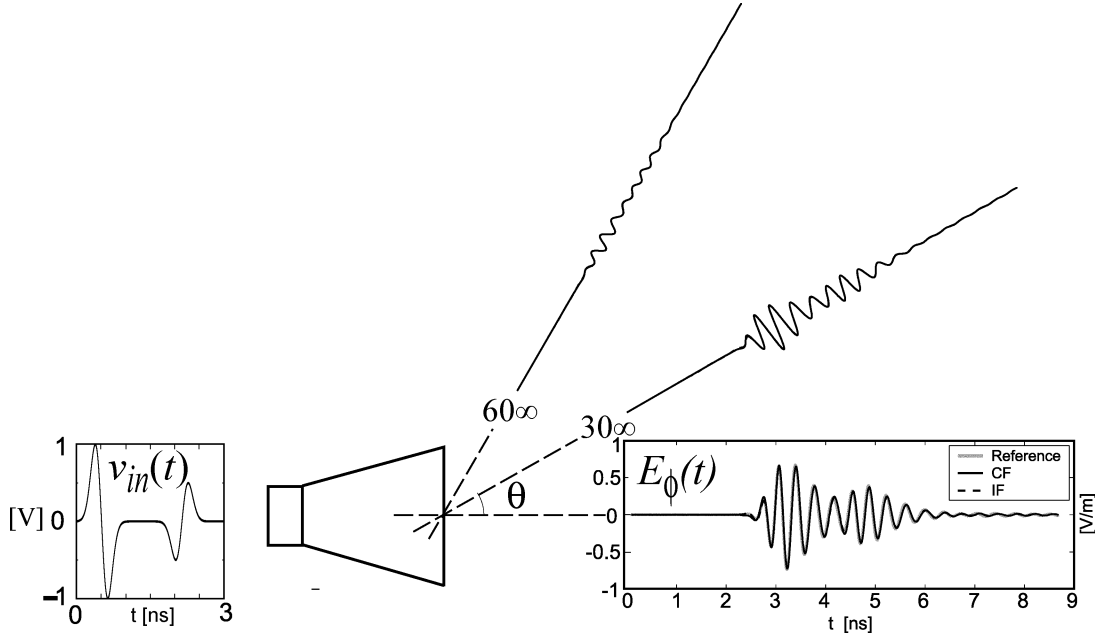


Fig. 9. Pyramidal ridged-horn: far field radiation at distance from the aperture $r = 31$ cm, computed by full FDTD and convolution in (1) when the input signal is a couplet of derivated Gaussian pulses.

formulas which mainly involve exponentials, the convolution with real input signals can be performed in a very efficient way. Finally, the developed semi-analytical formulas are well suited to be used together with a ray tracing for the characterization of UWB propagation in real indoor scenarios for any kind of signal coding.

APPENDIX

A. Details About the Definition of TD Aperture Effective Height

According to [18], the TD far-field radiation corresponding to $\mathbf{E}_a^\delta(\boldsymbol{\rho}, \tau)$ aperture field is

$$\mathbf{E}(\mathbf{r}, t) = \frac{1}{2\pi r c} \hat{\mathbf{r}} \times \frac{\partial}{\partial t} \iint_{S_a} \mathbf{E}_a^\delta \left(\boldsymbol{\rho}, t - \frac{r - \hat{\mathbf{r}} \cdot \boldsymbol{\rho}}{c} \right) ds \times \hat{\mathbf{z}}. \quad (\text{A.1})$$

Equalling (A.1) with (1) for $v_{in}(t) = 2R_g\delta(t)$, the expression of \mathbf{h}^T in (2) is formally obtained.

B. Calculation of the $\mathbf{h}_{p,\infty}^R$ Integral in (9)

For the case of a rectangular aperture of size $a \times b$, the integral in $\mathbf{h}_{p,\infty}^R$ is of the form

$$\psi(\tau) = \int_{-\frac{b}{2}}^{\frac{b}{2}} \int_{-\frac{a}{2}}^{\frac{a}{2}} \delta(\tau' + \alpha x + \beta y) f(x, y) dx dy \quad (\text{B.1})$$

with $\tau' = \tau - t_p$, $\alpha = c^{-1} \cos \phi \sin \theta$, $\beta = c^{-1} \sin \phi \sin \theta$ and $f(x, y)$ is any Cartesian component of the basis function \mathbf{e}_p . By using the properties of the Dirac function [19] and performing

integration with respect to x variable, the surface integral is reduced to the following line integral:

$$\psi(\tau) = \frac{1}{|\alpha|} \int_{y_1(\tau)}^{y_2(\tau)} f \left(-\frac{\tau'}{\alpha} - \frac{\beta}{\alpha} y, y \right) dy \quad (\text{B.2})$$

where the time-dependent integration limits are

$$y_1(\tau) = \max \left\{ -\frac{b}{2}, -\frac{\tau'}{\beta} - \frac{\alpha a}{2\beta} \right\} - \max \left\{ -\frac{b}{2} - \frac{\tau'}{\beta} - \frac{\alpha a}{2\beta}, 0 \right\} \quad (\text{B.3})$$

$$y_2(\tau) = \min \left\{ \frac{b}{2}, -\frac{\tau'}{\beta} + \frac{\alpha a}{2\beta} \right\} + \max \left\{ -\frac{b}{2} + \frac{\tau'}{\beta} - \frac{\alpha a}{2\beta}, 0 \right\}. \quad (\text{B.4})$$

Simpler expressions are anyway obtained for observation points along the principal cuts $\phi = \{0, \pi/2\}$. For instance, it is easy to show that in the case of $\phi = 0$ (B.1) becomes

$$\psi(t) = \begin{cases} \frac{c}{\sin \theta} \int_{-\frac{b}{2}}^{\frac{b}{2}} f \left(-\frac{c\tau'}{\sin \theta}, y \right) dy, & |\tau'| < \frac{a \sin \theta}{2c} \\ 0 & \text{otherwise.} \end{cases} \quad (\text{B.5})$$

As an example, the integral $\mathbf{h}_{p,\infty}^R$ at $\phi = 0$, corresponding to the TE₁₀ basis function $\mathbf{e}_p(\boldsymbol{\rho})_{10} = \sqrt{2/ab} \sin((\pi/a)x)\mathbf{y}$ is

$$\mathbf{h}_{10,\infty}^R(\hat{\mathbf{r}}, \tau) = -\frac{1}{\mu_0} \sqrt{\frac{2b}{a}} \sin \left(\frac{\pi c(\tau - t_p)}{\sin \theta} \right) \cot \theta \hat{\boldsymbol{\theta}}. \quad (\text{B.6})$$

ACKNOWLEDGMENT

The authors wish to thank Dr. P. Roselli, University of Rome "Tor Vergata," Rome, Italy, for support and discussions.

REFERENCES

- [1] R. J. Fontana, "Recent applications of ultra-wideband radar and communications systems," in *Ultra-Wideband Short-Pulse Electromagnetics 5*, P. D. Smith and S. R. Cloude, Eds. Norwell, MA/New York: Kluwer Academic/Plenum Publisher, 2000, pp. 225–234.
- [2] E. G. Farr and C. E. Baum, Extending the definition of antenna gain and radiation pattern into the time domain, in *Sensor and Simulation Notes*, Nov. 1992.
- [3] D. Lamensdorf and L. Susman, "Baseband-pulse-antenna techniques," *IEEE Antennas Propag. Mag.*, vol. 36, pp. 20–30, Feb. 1994.
- [4] O. E. Allen, D. A. Hill, and A. R. Ondreka, "Time domain antenna characterization," *IEEE Trans. Electromagn. Compat.*, vol. 35, pp. 339–345, 1993.
- [5] A. Shlivinski, E. Heyman, and R. Kastner, "Antenna characterization in the time domain," *IEEE Trans. Antennas Propag.*, vol. 45, no. 7, pp. 1140–1149, 1997.
- [6] B. Scheers, M. Acheroy, and A. Vander Vorst, "Time-domain simulation and characterization of TEM horns using a normalized impulse response," *IEE Proc. Microw. Antennas Propag.*, vol. 147, pp. 463–468, Dec. 2000.
- [7] W. Sorgel, C. Waldschmidt, and W. Viesbeck, "Electromagnetic characterization of ultra wideband antennas," in *Electromagnetics in a Complex World*, I. M. Pinto, V. Galdi, and L. B. Felsen, Eds. Berlin: Springer-Verlag, 2004, pp. 225–234.
- [8] D. V. Giri and C. E. Baum, Reflector IRA design and boresight temporal waveforms, in *Sensor and Simulation Notes*, Feb. 1994.
- [9] S. P. Skulkin and V. I. Turchin, "Transient field calculation of aperture antennas," *IEEE Trans. Antennas Propag.*, vol. 47, no. 5, pp. 929–932, May 1999.
- [10] A. Taflove, *Computational Electrodynamics: The Finite Difference Time Domain Method*. Norwood, MA: Artech House, 1995.
- [11] G. Marrocco, "Modal near-field to far-field transformation for FDTD modeling of aperture antennas," *J. Electromagn. Waves Appl.*, vol. 17, no. 1, pp. 79–98, 2003.
- [12] G. Marrocco and M. Ciattaglia, "Ultrawide-band modeling of transient radiation from aperture antennas," *IEEE Trans. Antennas Propag.*, vol. 52, no. 9, pp. 2341–2347, Sep. 2004.
- [13] C. E. Baum, "The singularity expansion method," in *Transient Electromagnetic Fields*, L. B. Felsen, Ed. Berlin: Springer-Verlag, 1976.
- [14] A. Poggio, M. Van Blaricum, E. Miller, and R. Mittra, "Evaluation of a processing technique for transient data," *IEEE Trans. Antennas Propag.*, vol. 26, no. 1, pp. 165–173, Jan. 1978.
- [15] G. Marrocco and F. Bardati, "Time-domain macromodel of planar microwave devices by FDTD and moment expansion," *IEEE Trans. Microwave Theory Tech.*, vol. 49, pp. 1321–1328, 2001.
- [16] T. K. Sarkar and O. Pereira, "Using the Matrix Pencil method to estimate the parameters of a sum of complex exponentials," *IEEE Antennas Propag. Mag.*, vol. 37, no. 1, pp. 48–55, 1995.
- [17] W. H. Press, S. Teukolsky, W. T. Vetterling, and B. P. Flannery, *Numerical Recipes in C—the Art of Scientific Computing*. Cambridge, U.K.: Cambridge Univ. Press, 1992.
- [18] T. B. Hansen and A. D. Yaghjian, "Planar near-field scanning in the time domain, part 1: formulation," *IEEE Trans. Antennas Propag.*, vol. 42, pp. 1280–1291, 1994.
- [19] E. W. Weisstein, *CRC Concise Encyclopedia of Mathematics*. London, U.K.: Chapman & Hall, 1969, pp. 129–179.



Matteo Ciattaglia (S'02) received the Laurea degree in telecommunication engineering at the the University of Rome "Tor Vergata," Rome, Italy, in 2002, where he is currently working toward the Ph.D. degree.

In the 2003, he was Grant Researcher at the University of Rome "Tor Vergata," working on numerical methods for time-domain electromagnetics. He is currently employed at Alenia Marconi Systems, Rome, Italy, working on phased arrays modeling.



Gaetano Marrocco (S'96–M'98) received the Laurea degree in electronic engineering and the Ph.D. degree in applied electromagnetics from the University of L'Aquila, L'Aquila, Italy, in 1994 and 1998, respectively.

Since 1997, he has been a Researcher at the University of Rome "Tor Vergata," Rome, Italy, where he currently teaches antenna design and bioelectromagnetics. In summer 1994, he was at the University of Illinois at Urbana-Champaign as Postgraduate Student. In autumn 1999, he was a Visiting Researcher at the Imperial College in London, London, U.K. He has been involved in several space, avionic and naval programs of the European Space Agency, NATO, Italian Space Agency, and the Italian Navy. His research is mainly directed to the development of numerical methods and signal processing techniques for the time domain modeling of complex electromagnetic structures in the context of biological and aerospace applications.